PERGAMON

International Journal of Heat and Mass Transfer 41 (1998) 4297–4313

International Journal of HEAT and MASS TRANSFER

Mean structure in the viscous layer of strongly-heated internal gas flows. Measurements

A. Mohsen Shehata[a], Donald M. McEligot[b,c,*]

[a] *Xerox Corporation, MS W111-20N, Webster, NY 14580, U.S.A.*
[b] *Aerospace and Mechanical Engineering Department, University of Arizona, Tucson, AZ 85721, U.S.A.*
[c] *Idaho National Engineering and Environmental Laboratory/Lockheed Martin Idaho Technologies Co., Idaho Falls, ID 83415-3885, U.S.A.*

Received 20 February 1996; in final form 24 February 1998

Abstract

Experiments for air flowing upward in a vertical circular tube were conducted for heating rates causing significant property variation in primarily forced convection. Two entry Reynolds numbers were employed, concentrating on three heating rates of $q_i^+ = q''_w/Gc_{p,in}T_{in} \approx 0.0018$, 0.0035 and 0.0045, to give conditions considered to be 'turbulent', 'sub-turbulent' and 'laminarizing'. In addition to variation of integral parameters, results include the mean velocity and temperature distributions—needed to guide development of advanced turbulence models for this situation. However, comparison to a simple approach—a modified version of the van Driest model—shows useful agreement. © 1998 Published by Elsevier Science Ltd.

Nomenclature

$\{\}$ function of
c_p specific heat at constant pressure
D tube inside diameter
$\boldsymbol{g}$ acceleration of gravity
g_c units conversion factor, e.g., 1 kg m (N^{-1} s^{-2})
G mean mass flux, $4\dot{m}/\Pi D^2$
h convective heat transfer coefficient
k thermal conductivity, turbulent kinetic energy
l, l mixing length
L turbulent length scale
$\dot{m}$ mass flow rate
p pressure
q'' heat flux; q''_w, wall heat flux
r radius; r_w, tube wall radius
T absolute temperature; t, relative temperature
u streamwise velocity component; U, time-mean streamwise velocity component
u_τ friction velocity, $(g_c\tau_w/\rho_w)^{1/2}$
v radial velocity component; V, time-mean radial velocity component
V_b bulk or mixed-mean streamwise velocity
x axial location, measured upward from start of heating
y coordinate perpendicular to the wall.

Greek symbols

ε eddy diffusivity, ε_m for momentum, ε_h for thermal energy; dissipation
μ absolute viscosity
ν kinematic viscosity
ρ density
τ shear stress; τ_w, wall shear stress.

Subscripts

b evaluated at bulk or mixed-mean temperature (or enthalpy)
c centerline
eff effective
fd fully developed (velocity) or fully established (heat transfer)
i, in inlet
m mixed-mean or bulk, also peak value
v evaluated at location where $\varepsilon = \nu$, relates to viscous layer length scale
w wall, evaluated at wall temperature
x evaluated at local axial position.

* Corresponding author.

0017–9310/98 $19.00 © 1998 Published by Elsevier Science Ltd.
PII: S0017-9310(98)00088X

Non-dimensional quantities

A^+ constant or function in van Driest mixing length model

f friction factor, $2\rho_b g_c \tau_w / G^2$

Gr_q local Grashof number based on heat flux, $\boldsymbol{g} D^4 q''_w / (\nu_b^2 k_b T_b)$

K_V acceleration parameter, $K_V = (\nu_b / V_b^2)(\mathrm{d}V_b/\mathrm{d}x)$

Nu Nusselt number, e.g., hD/k

P^+ pressure defect, $\rho_{in} g_c (p_{in} - p)/G^2$

Pr Prandtl number, $c_p \mu / k$; Pr_t, turbulent Prandtl number, $\varepsilon_m / \varepsilon_h$

q^+ heat flux, $q''_w / G c_p T$; q_i^+, based on inlet conditions, $q''_w / G c_{p,in} T_{in}$

Re Reynolds number, $4\dot{m}/\Pi D \mu$; $Re_{w,m}$, modified wall Reynolds number, $V_b D / \nu\{T_w\}$

St Stanton number, $h / G c_p$

t^+ temperature, $(T_w - T)\rho_w u_{\tau,w} c_{p,w} / q''_w$

u^+ streamwise velocity component, U/u_τ

y^+ wall distance, $y(g_c \tau_w / \rho_w)^{1/2} / \nu_w$; y_v^+, predicted viscous layer thickness.

1. Introduction

For dominant forced convection with significant gas property variation, in low Mach number flow of common gases through a circular tube, apparently the only published internal profile data available to guide (or test) the development of predictive turbulence models are K. R. Perkins' measurements of mean temperature distributions [1]. The work here takes the next step: the first mean velocity distributions for this situation are presented.

A wide variety of basic studies has been conducted examining turbulence structure in simple boundary layers with constant properties; but almost none have been accomplished for accelerating flows with significant transport property variation as induced by strong heating of a gas in internal flow, e.g., inside a circular tube. These flows develop continuously downstream. There are several phenomena that relate to the flow development: thickening of the viscous sublayer, flow acceleration and buoyancy effects for example.

In our terminology, the viscous layer is operationally defined to include both the so-called 'linear' layer, where molecular effects dominate, and the next region where molecular effects are still significant but not dominant. For unheated flows, these regions typically extend to y^+ of about five and thirty, respectively. This usage follows that suggested by Bradshaw [2] (and contrasts with another popular common definition where the linear region is called the viscous layer [3]).

It is probably also appropriate to point out that the use of resistive heating, as in the present experiment, poses a severe challenge for turbulence models. An approximately constant wall heat flux evolves. With significant property variation due to large temperature ratios, it is easier to model turbulent flows with constant wall temperature as the boundary condition than those with a specified wall heat flux. With a constant wall temperature, the fluid properties in the viscous region do not change substantially in the axial direction. With a constant or increasing wall heat flux, the transport properties in the viscous region change continuously and rapidly for strong heating rates as the flow progresses downstream.

In experiments,the attempt to obtain some reasonable spatial resolution for the dominant viscous layer while measuring mean velocity and temperature distributions in strongly heated, internal gas flows leads the experimenter to flirt with laminar flow and its approach, called 'laminarization' [4] or 'reverse transition' [5]. For this latter situation, a tube flow turbulent at its inlet gradually begins to approach results corresponding to laminar theory (in terms of integral parameters, such as local Nusselt numbers and local skin friction coefficients) although turbulent fluctuations are usually still evident. For further general background on laminarization in internal convective heat transfer to gases, a survey by McEligot [6] may be useful.

The present data are for gas flows where forced convection dominates. From a developed turbulent flow at a nominal room temperature, the maximum heating rate yields maximum wall temperatures of about 840 K; but the 27 mm diameter tube is small enough that mixed convection parameters indicate that buoyancy effects would be small. These measurements further supplement and extend earlier data for internal turbulent flows in small tubes ($D < 13$ mm $\approx 1/2$ inch) with temperature-dependent transport properties that could only provide integral parameters, e.g., by Humble, Lowdermilk and Desmon [7], Jackson [8], McEligot, Magee and Leppert [9], Perkins and Worsoe-Schmidt [5] and others. These earlier data gave initial tests of turbulence models accounting for temperature-dependent transport properties, as demonstrated by McEligot and Bankston [10], Bankston and McEligot [11] and Kawamura [12].

By comparison to thermal entry measurements, Bankston and McEligot [11] were able to examine the application of eleven algebraic turbulence models for high-Reynolds-number turbulent gas flows with properties varying strongly in both axial and radial directions. Best agreement was found with a van Direst mixing length model [13] with the exponential term evaluated with wall properties. To accommodate low-Reynolds-number turbulent and laminarizing flows, McEligot and Bankston [10] modified this model as described later in Section 2. This modification was developed by comparison to integral quantities, such as the local Stanton number, since internal profile measurements were not then available for guidance.

To provide internal data, Perkins [1, 14] conducted

experiments to obtain mean axial and radial temperature distributions in strongly-heated turbulent and laminarizing flows with dominant forced convection. Conditions were categorized as turbulent, laminarizing or subturbulent (or intermediate). After adding a body force term to the axial momentum equation in the computer program of Bankston and McEligot [11, 15], data were compared to predictions. Perkins and McEligot concluded that simple modifications of the van Driest model predicted the trends of local Nusselt numbers and the mean temperature profiles well for turbulent flows and for flows laminarizing rapidly, but that the 'subturbulent' flows were more difficult to simulate.

Most recent work on the topic of laminarization by heating has been conducted in Japan. Measurements of local heat transfer coefficients and friction factors for transitional and laminarizing flows have been obtained by Ogawa et al. [16] and Ogawa and Kawamura [17] with circular tubes. Local Nusselt numbers were measured for annuli by Fuji et al. [18] and Torii et al. [19]. The first investigator to succeed in applying an 'advanced' turbulence model to laminarization by heating apparently was Kawamura [12]. He concluded that a modified k–kL model gave good agreement with the experiments. Ogawa and Kawamura [17] also observed that the k–kL model predicted their local friction factor data well during laminarization. Fujii et al. [18] employed three types of turbulence models for comparisons to their measurements of strongly-heated turbulent gas flow in an annulus. Torii et al. [19] and Torii and Yang [20] applied a modified k–ε model for predicting streamwise variation of heat transfer parameters in low-Reynolds-number turbulent and laminarizing flows in circular tubes and annuli. Torii et al. [21] also attempted to apply the Reynolds-stress model of Launder and Shima [22] to $St\{Re\}$ data for a circular tube; they concluded that predictions were comparatively poor in the range of turbulent-to-laminar transition.

None of these investigators appear to have compared their predictions to internal data for strongly-heated gas flows. To the authors' knowledge, the only numerical studies of 'advanced' turbulence models for turbulent and laminarizing flows at high heating rates that utilized internal data have been those of Mikielewicz [23], Ezato et al. [24] and Nishimura et al. [25] which employed measurements from the present study.

The general goal of the present study is to obtain greater understanding of the structure of strongly heated, internal, turbulent gas flows and their 'transition' to apparent laminar flows, with the current emphasis being on mean structure. Accordingly, the immediate objective is to measure the development of distributions of the mean streamwise velocity and temperature in a well-defined, axisymmetric experiment involving significant variation of the gas transport properties in the viscous layer, which dominates convective thermal resistance. A second objective is to document the data so they can be used to test hypothesized turbulence models and proported 'general purpose', computational thermal fluid dynamic codes. Some advanced methods use 'parabolic sublayers' based on mixing length models near the wall to reduce computer storage requirements and calculation times for complex flows or geometries (or complex models); therefore an additional objective is to examine the validity of the modified van Driest mixing length model of McEligot and Bankston [10] that was derived to account for property variation in the viscous layer due to high heating rates. Flow rates and heating rates were chosen to yield experimental conditions leading to results which range from predominantly turbulent to near laminar flow in integral terms.

2. Predictive technique

The numerical method employed was the finite-control-volume approach of Bankston and McEligot [11] as modified by Bates et al. [15] to include a body force term in the x-momentum equation to account for buoyancy effects,

$$\rho U\frac{\partial U}{\partial x}+\rho V\frac{\partial V}{\partial r}+g_c\frac{\mathrm{d}p}{\mathrm{d}x}+\rho \boldsymbol{g}=\frac{1}{r}\frac{\partial}{\partial r}\left(r\mu_{\mathrm{eff}}\frac{\partial U}{\partial r}\right).$$

Other governing equations remain as presented by Bankston and McEligot. Basic assumptions implied include axisymmetric steady mean flow at a low Mach number with steady heating. Internal boundary layer approximations are used in derivation of the governing continuity, x-momentum, energy and integral continuity equations. No changes of phase or chemical composition are accommodated. Many authors neglect the density variation in the convective terms (i.e., the so-called Boussinesq approximation) but density variation is treated in all terms in the present work. Details of the iterative solution procedure are presented in the paper by Bankston and McEligot. The effective viscosity is evaluated via a mixing length approach with

$$\mu_{\mathrm{eff}}=\mu+\mu_t \quad \text{and} \quad \mu_t=\rho l^2|\partial U/\partial r|.$$

The viscosity, density and mean velocity gradient are evaluated at their pointwise values.

Initial conditions are specified at the entry; these are taken well upstream from the start of heating when the experiment utilizes an 'adiabatic' hydrodynamic entry of constant diameter, as in the present experiment. The wall is impermeable and investigators' tabulations of local wall heat fluxes are approximated by spline functions for the thermal boundary condition in the heated region. Mesh spacing is varied in both the radial and axial directions. To treat the variation of transport properties through the viscous layer, the first point of calculation in the radial direction is at $y^+\approx 0.5$ or less. Mesh par-

ameters are adjusted to give heat transfer and wall friction results within about one per cent of converged values.

In the present work, the transport properties of air are represented by power laws and the perfect gas approximation [1, 26] as $\rho \approx \rho_{in}(p/p_{in})(T_{in}/T)$, $\mu \approx \mu_{in}(T/T_{in})^{0.67}$, $k \approx k_{in}(T/T_{in})^{0.805}$ and $c_p \approx c_{p,in}(T/T_{in})^{0.095}$. The turbulence model is entered as a subroutine with effective viscosity and thermal conductivity formed as the sums of molecular and turbulent contributions.

As noted, an additional objective of the present study is to examine the validity of the simple, modified van Driest model [10] which was derived to account for property variation due to high heating rates in low-Reynolds-number gas flows. Based primarily on comparison to $St\{x\}$ data from small tube experiments. McEligot and Bankston extended the van Driest model to treat turbulent-to-laminar transition due to strong heating. Essentially, they extended a history/delay function with rate equations for integral parameters from Nash and MacDonald [27] and modified the van Driest representation to include Reynolds number dependence. McEligot and Bankston wrote their version of such a rate equation with the mixing length l as the dependent variable and hypothesized the rate of axial readjustment to vary with the pointwise shear stress and inversely with the viscosity as follows

$$\frac{\partial l\{x,y\}}{\partial x} = C\frac{\sqrt{\tau\{y\}/\rho\{y\}}}{\nu\{y\}}[l_{fd}\{x,y\} - l\{x,y\}].$$

The quantity l_{fd} represents the mixing length which would exist at the same conditions if a fully developed situation were possible. Large values of C represent rapid readjustment. Small values inhibit adjustment from the mixing length profile existing at the start of heating. The present calculations take $C = 0.001$ when $l > l_{fd}$ and $C = 0.0004$ when $l_{fd} > l$. For use in the numerical program the rate equation is integrated locally, with all variables except l treated as constant over the short distance, to give

$$l_{i,j} = l_{fd,i-1,j} - [l_{fd,i-1,j} - l_{i-1,j}]\exp\{-C\Delta x^+\}$$

where $x^+ = x[g_c\tau\{y\}/\rho\{y\}]^{1/2}/\nu\{y\}$ and i and j are indices for the mesh points.

For heat transfer to gases flowing turbulently at low Reynolds numbers and constant property conditions, Reynolds, Swearingen and McEligot [28] had successfully correlated their quantity y_1^+ as a function of Reynolds number to predict friction factors, local Nusselt numbers and adiabatic velocity profiles adequately. Accordingly, McEligot and Bankston adjusted the constant in the van Driest model to become a function $A^+\{Re\}$, since constant property predictions from the van Driest model become poor in the low-Reynolds-number range [29]. For flows with significant property variation, it is not evident which possible definition of the local Reynolds number is appropriate to use in the function. For the present work we chose the modified wall Reynolds number, $Re_{w,m}$ $(= V_b D/\nu\{T_w\} = Re\ (\nu_m/\nu_w))$, since—in comparisons to laminarizing data—McEligot and Bankston found that employing $A^+\{Re_{w,m}\}$ lead to slightly conservative results for heating. Thus, in the present numerical calculations, the quantity l_{fd} is evaluated as

$$l_{fd} = \kappa y[1 - \exp(-y^+/A^+\{Re_{w,m}\})]$$

with the wall coordinate y^+ specifically defined as $y[g_c\tau_w/\rho_w]^{1/2}/\nu_w$ [11]. The function $A^+\{Re_{w,m}\}$ which was used in the present work is listed in Table 1; a value of 0.4 is used for κ. The original paper [10] and the review by McEligot [6] provide further discussion of the philosophy leading to this simple, modified model and of some unsuccessful alternate attempts.

To evaluate the effective thermal conductivity, Reynolds analogy (i.e., $\varepsilon_h = \varepsilon_m$ or $Pr_t = 1$) is used. In addition to being convenient, this approach has recently been shown to be as effective—for predicting $Nu\{x\}$ in flows of low-Prandtl-number gas mixtures—as any of a popular variety of models for the turbulent Prandtl number and Direct Numerical Simulation [30]. Comparison to the present measurements will indicate whether it is acceptable for predicting internal mean profiles with strong property variation.

3. Experiment

The experimental objective of Shehata [26, 31] was to measure the distributions of the mean streamwise velocity and temperature for dominant forced convection in a well-defined, axisymmetric experiment involving significant variation of the gas transport properties across the viscous layer. Accordingly, experiments were conducted for air flowing upwards in a vertical circular tube

Table 1
The function $A^+\{Re_{w,m}\}$ [10]

$Re_{w,m}$	$A^+\{Re_{w,m}\}$
<2225	1×10^{10}
2225	1250
2560	64
3000	54
4000	47
9000	37
14 500	34
44 000	30
80 000	28.5
5×10^5	27

heated resistively; the desired internal distributions were determined via hot wire anemometry.

A reason for the paucity of data in the available literature—for profiles in dominant forced convection of common gases with high heating rates—tends to be related to size. The region controlling the transfer of heat and momentum in turbulent wall flows is primarily the viscous layer which occupies a small fraction of the cross section. This fraction grows as the Reynolds number is lowered. With strong heating, the large turbulent temperature fluctuations make simultaneous measurement of instantaneous temperature and velocity desirable—but available multisensor probes generally do not provide the spatial resolution necessary without 'large' size. However, if one chooses a large tube and a low Reynolds number (for thicker viscous layers) to improve spatial resolution, the problem quickly becomes one of dominant natural convection. The experimenter must compromise in order to obtain data which the theorist can extend to conditions where the experimenter cannot easily tread.

The experiment was conducted in an open loop built around a vertical, resistively-heated, circular test section exhausting directly to the atmosphere in the laboratory. The experiment was designed to approximate a uniform wall heat flux to air, entering with a fully-developed turbulent velocity profile at a uniform temperature. Small single wire probes were introduced through the open exit in order to obtain pointwise temperature and velocity measurements. Details of the experiment plus tabulations of resulting data are available in a report by Shehata and McEligot [31] with some additional information given by Perkins [1].

A resistively-heated, seamless, smooth, extruded Inconel 600 tube of 27.4 mm (1.08 in.) inside diameter was employed as the test section. Heated length between the electrodes was about 32 diameters and it was preceded by a 50 diameter, unheated entry region for flow development; the short heated length was picked to permit high heating rates with this material while possibly approaching quasi-developed conditions. Outside wall temperatures were determined with premium grade, Chromel Alumel thermocouples distributed along the tube. The axial variation of the static pressure was obtained with pressure taps electrostatically drilled through the wall.

A single hot wire sensor was chosen to measure the streamwise velocity and temperature, in preference to an X-probe or other multiple sensor probe, in order to minimize flow disturbances and blockage by prongs and support in the 27 mm tube and to permit measurements closer to the wall. It was employed as a hot wire for velocity measurements and as a resistance thermometer for pointwise temperatures. In addition to the usual difficulties of hot wire anemometry, the temperature range of the present experiment introduced additional problems. These difficulties, their solutions and related supporting measurements are described by Shehata [26, 31].

Convective and radiative heat losses from the outside of the tube were reduced by insulating with a 13 mm (1/2 in) thick layer of fine silica bubbles, surrounded in turn by electrical heating tapes for guard heating. By this method, heat losses were constrained to less than 10% of the thermal energy generation rate except within a few diameters of the electrodes; the heat losses were calibrated so the consequent uncertainties in $q''_w\{x\}$ were considerably less than the heat loss magnitudes. Confidence tests included checking the mean velocity profiles and their symmetry in adiabatic flow runs at Reynolds numbers about 4000, 6000 and 8000. Adiabatic skin friction coefficients were calculated from static pressure differences between a location near the nominal start of heating (x/D defined to be zero) and $x/D \approx 19.7$ for Reynolds numbers from about 3000–10 000. These data fell between accepted correlations for fully-developed turbulent flow: those of Blasius [32] and of Drew et al. [33]. They agreed to within 1–2%.

Experimental uncertainties were estimated employing the technique of Kline and McClintock [34]. Examples of the resulting uncertainties in velocity and temperature are tabulated as functions of position and experimental run by Shehata [26]. In general, the uncertainty in velocity was calculated to be in the range of 8–10% of the pointwise value, with the larger percent uncertainties occurring near the wall. The uncertainty in temperature was typically 1–2% of the pointwise absolute temperature. These estimates are believed to be conservative (i.e., pessimistic) since comparisons of the integrated and measured total mass flow rates for each profile showed better agreement—of the order of 3% or less, except near the exit in the runs with the two highest heating rates. The estimated experimental uncertainty in the Stanton number was 6% or less for the range $3 < x/D < 20$ and for the non-dimensional pressure defect it was about 4% at the last measuring station [1].

4. Results

4.1. Range of variables

Experimental conditions were selected to correspond to three generic situations: (1) essentially turbulent flow with slight, but significant, air property variation, (2) severe air property variation evolving to near laminar flow (as implied by the integral heat transfer parameters) and (3) moderate gas property variation, yielding behavior that was intermediate or transitional between the first two. Perkins [1] had found that the thermal development of the latter situation was the most difficult of the three to predict. Inlet Reynolds numbers of about

6080, 6050 and 4260 with non-dimensional heating rates, q^+, of about 0.0018, 0.0035 and 0.0045, respectively, yielded this range. Over the range $5 < x/D < 26$ the wall heat flux was uniform to within 3% of the average value. Inlet temperature was about 24°C (75°F).

The length of the test section was chosen to permit measurements through and beyond the normal thermal entry region while attaining significant transport variation, as exemplified by T_w/T_b and T_w/T_i, with common materials and gas. Wall temperatures reached 850 K (1510R), maximum wall-to-bulk temperature ratio was about 1.9 and the Mach number was less than 0.013, indicating that compressibility effects would have been negligible. At the entrance the buoyancy parameter Gr_q/Re^2 reached 0.53 for the highest heating rate and lower Reynolds number. The maximum wall-to-inlet temperature ratio was about 2.7, indicating that gas properties such as viscosity varied by a factor of two in the test section.

For the thermal entry comparisons shown herein, the deduced wall heat flux variation $q''_w\{x\}$ of the experiments was employed as the boundary condition in the predictions, starting at $x = 0$, rather than the usual constant-heat-flux idealization. Electrical resistance heating of the test section, as in this experiment, yields an axial heat flux distribution near the electrode that may be approximated as exponentially approaching a constant value at small axial distances. Reynolds et al. [28] provide an eigenvalue solution for the exponential description; for their low-Reynolds-number data this analytical solution approaches the comparable solution based on the constant-wall-heat-flux idealization to within 2% before four diameters.

4.2. Axial variation of integral parameters

The streamwise variations of some of the pertinent integral parameters are shown in Fig. 1. These quantities were deduced with the aid of energy balances which accounted for radial heat loss through the insulation, axial conduction along the test section to the electrodes and the slight variation of the electrical resistivity. The individual runs are identified by three digits representing the inlet Reynolds number and the non-dimensional heating rate (e.g., Run 635 is for $Re_i \approx 6000$ and $q^+ \approx 0.0035$).

The first subfigure compares the measured wall temperatures. After the immediate thermal entry the wall temperature varies almost linearly despite the property variation; this behavior is comparable to the case with constant properties and constant wall heat flux [35] but the magnitudes differ. One sees that the unheated entry region is not completely adiabatic at these high heating rates due to axial thermal conduction in the Inconel tube and axial thermal radiation from the internal wall temperature downstream. The bulk temperature variation is nearly linear in these experiments because the wall heat flux and the specific heat of the air are both almost constant.

The bulk Reynolds number, Re_m, decreases up the tube as a consequence of the increasing bulk temperature and viscosity. However, even for the most severe case it is not as low as 3000, which is still well above the value for transition in long tubes, according to conventional wisdom.

The local buoyancy parameter, Gr_q/Re_m^2, behaves in an unexpected but explicable manner. (For evaluation of this parameter, properties are taken at the local bulk temperature, e.g., $q^+_{x,m}$ is defined as $q''_{w,x}/(G_{cp,b}T_b)$.) The numerator remains constant for a gas with constant heat flux, while the denominator increases as $T^{3.8}$, approximately. Consequently, this parameter is highest near the thermal entrance and then decreases along the test section. The maximum values indicate that buoyancy effects could be noticeable—and, in predictive techniques, must be treated in the momentum equation at least and possibly in the turbulence model directly. Mikielewicz et al. [29] have examined the possible effects on the present data and concluded that buoyancy would have affected the Nusselt number by 7% or less in the worst case.

The local acceleration parameter, K_V, remained near constant after the immediate thermal entry, except for the last few diameters near the exit. It reached values of 1.2×10^{-6}, 2.2×10^{-6} and 4×10^{-6} for runs 618, 635 and 445, respectively. For unheated accelerating flows, Kline et al. [36] noted that turbulent bursts apparently ceased when their comparable K_u reached a critical value of 3.7×10^{-6}. On the other hand, for a value of K_V of about 1.5×10^{-6} Chambers et al. [37] found the bursting rate to remain approximately constant at the turbulent value when based on wall scaling. In these terms, the present experiments could be expected to span a range from fully turbulent to 'laminarizing'.

For the thermal design engineer, the first test of a predictive technique typically is the Nusselt number. Figure 1(e) provides our measurements and predictions based on the modified van Driest model. Run 618 shows typical thermal entry behavior for a turbulent flow—the thermal entry extends to about 15–20% diameters and then the Nusselt number levels. However, downstream the Nusselt number is about 20% lower than the constant properties prediction for the same conditions, as expected for the effect of property variation. Typical empirical correlations account for this reduction as approximately $(T_w/T_b)^{-1/2}$ which would give a reduction of about 16% in this case [9]. For Run 635 at the same entering Reynolds number, the data in the thermal entry are approximately the same but downstream the Nusselt number decreases continually. This decrease is partly because the Reynolds number decreases further with the higher heating rate; compared to a turbulent constant properties correlation,

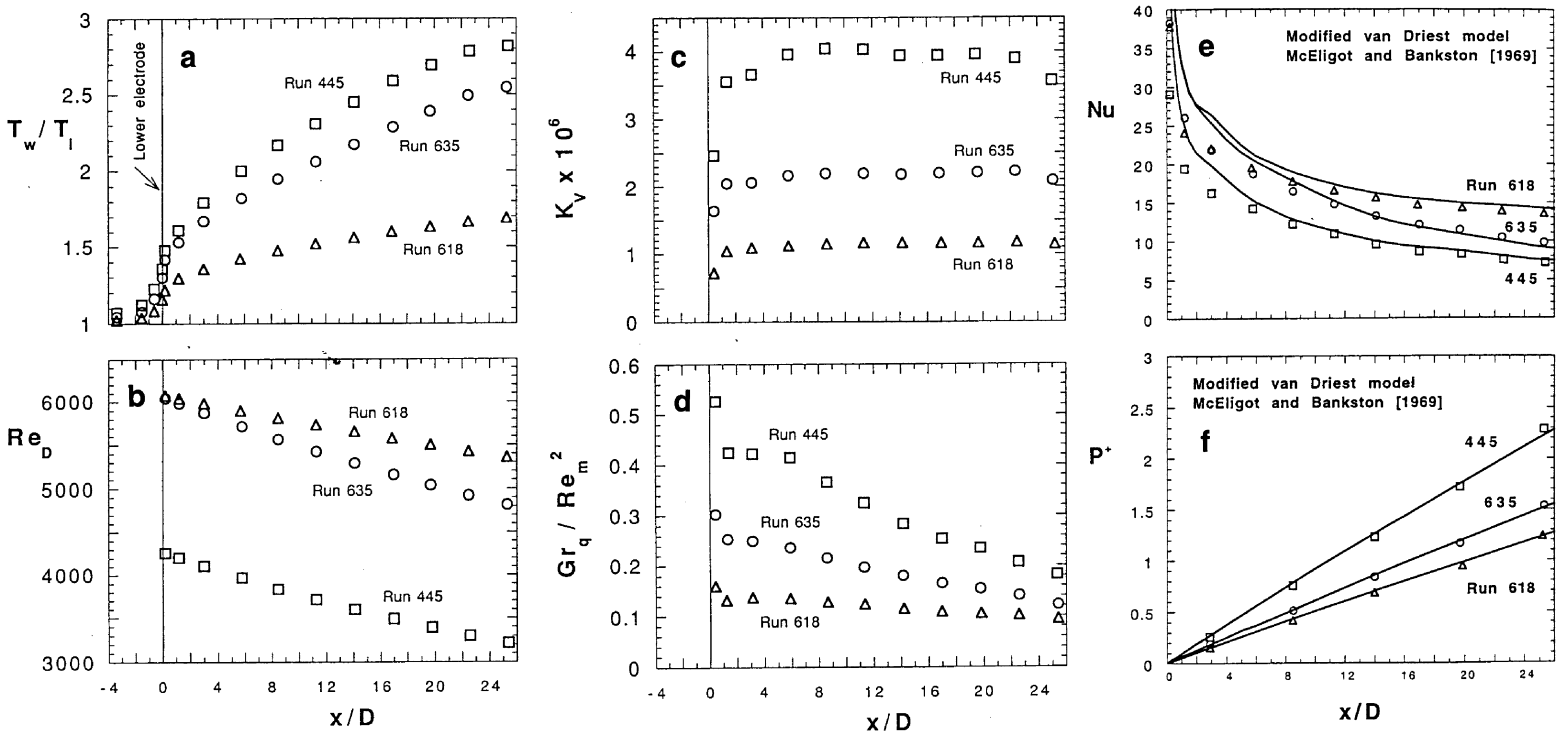

Fig. 1. Axial distributions of integral parameters. (a) Wall temperature. (b) Local bulk Reynolds number. (c) Acceleration parameter. (d) Buoyancy parameter. (e) Local bulk Nusselt number. (f) Pressure defect (non-dimensional pressure decrease).

Nu is about 45% low at 25 diameters while a turbulent variable properties correlation would suggest only a 30% reduction. Thus, this run might be considered to be laminarizing downstream.

Run 445 is for a lower entering Reynolds number than the other two and, consequently, the data are lower in the thermal entry; they then continue to decrease downstream. As shown by Shehata [26], these values diverge from a turbulent correlation and begin to agree with the analytic correlation of McEligot and Swearingen [38] for purely laminar flow with property variation; for example, at $x/D \approx 25$ the data are about equidistant from the turbulent and laminar variable-property predictions at about 20% difference from each, but are diverging from the former and converging on the latter. Yet Fig. 1(b) shows Re_m to be still above 3200 at this location.

For $x/D > \sim 8$, the modified van Driest model predicts $Nu\{x\}$ quite well. This form of presentation emphasizes the differences between predictions and data at low axial distances whereas comparison of $Nu\{Re\}$ or $St\{Re\}$ hides these discrepancies. The principal cause of the difference at low x/D is the difference in thermal boundary condition: the apparatus has thermal conduction upstream from the first electrode via the test section wall while the calculations approximate the boundary condition at $x = 0$ as a step change to an exponential approach to the (experimentally measured) near-constant $q''_w\{x\}$. Consequently, in the analysis *Nu* approaches infinity as $x \to 0$, but in the actual measurements *Nu* is finite there since a slight thermal boundary layer began upstream of the electrode. Shumway [39] demonstrated this situation for laminar flow. This preheating of the incoming flow introduces a fixed error in $T_b\{x\}$ so its percentage effects on $(T_w - T_b)$ and *Nu* decrease with increasing x/D. Shumway [40] estimated the order-of-magnitude of the preheating for Run 618 to be about 1% in terms of $\Delta T_b/T_i$; for this case the effect on *Nu* would decrease to about 2% by $x/D \approx 10$. For more precise predictions, one could solve the governing equations upstream with $T_w\{x\}$ specified from the experimental measurements as by Shumway [39] and then switch to the measured distribution of $q''_w\{x\}$ at $x/D = 0$. The necessary data for $T_w\{x\}$ are demonstrated in Fig. 1(a) and are tabulated in a report by Shehata and McEligot [31].

The second test for the thermal designer is how well the pressure drop is predicted. A direct comparison is given by the non-dimensional pressure defect, P^+. For strongly heated gas flow this comparison should not be a particularly severe test to meet since, the higher the value of q^+, the more the pressure drop due to acceleration dominates over wall friction and elevation change [24]; it becomes a test of the energy balance. For run 618 the wall shear stress contributes about half of the pressure drop while at the higher heating rate of run 445 it represents only about one-third. Figure 1(f) demonstrates that the modified van Driest model predicts $P^+\{x\}$ well for the turbulent, subturbulent and laminarizing conditions.

4.3. Downstream comparisons

Mean velocity and temperature profiles for the various runs are compared to each other for the viscous layer in Fig. 2 for $x/D \approx 14$ and 25, i.e., after the immediate thermal entry. The temperature profiles correspond to those of Perkins [1] while the velocity profiles are the major new contributions of the current work. Their shapes are also compared to conventional predictions for fully-established, constant-property, forced convection at $x/D \approx 25$, the furthest location downstream. To present profiles in terms of well-defined wall coordinates, $y_w^+ = yu_{\tau,w}/\nu_w$, $u_w^+ = U/u_{\tau,w}$ and $t_w^+ = (T_w - T)\rho_w u_{\tau,w} c_{p,w}/q''_w$, one needs a reasonable value of the friction velocity, $u_{\tau,w} = [g_c\tau_w/\rho_w]^{1/2}$. Direct measurements of the local wall shear stress are generally not feasible for the conditions of this experiment (and it cannot be deduced from local estimates of dp/dx as in unheated flow since $u\{y\}$ varies continuously in the streamwise direction). Conventional approaches and correlations will not provide reliable values. Here, $u_{\tau,w}$ is deduced from a combination of the measurements and the numerical predictions.

After a turbulence model has been adjusted so that the predicted profiles of $U\{y, x\}$ and $T\{y, x\}$ in the viscous layer agree with their measured values across and along the test section, then the values of τ_w from the program output can be taken as indirectly deduced data. The validity of the approach hinges on how well the predictions agree with the measurements; this comparison is presented in Sections 4.4 and 4.5 later. The pertinent code result is f_s/f_{DKM}, where f_s is the friction factor defined unambiguously in terms of bulk properties, and it is referenced to the Drew, Koo and McAdams correlation [33] here evaluated at the bulk Reynolds number (as in the code). The wall coordinates are defined in terms of fluid properties evaluated at the wall temperature, $\mu_w = \mu\{T_w\}$, $c_{p,w} = c\{T_w\}$ and so forth, as by Bankston and McEligot [11]. Once these properties are evaluated and τ_w is determined via $f_s = (f_s/f_{DKM}) \cdot f_{DKM}$, calculation of u_τ, y_w^+, u_w^+ and t_w^+ from their definitions is straightforward. The approach could be considered to be philosophically comparable to the technique of fitting data with a Clauser plot, but a Clauser plot is not valid for low Reynolds numbers or for flows changing significantly in the axial direction.

Temperature profiles show the trends identified by Perkins. These trends are slight at $x/D \approx 14$ where the thermal boundary layer has apparently barely reached the centerline and are more evident at $x/D \approx 24$ where there has been more opportunity for development in response

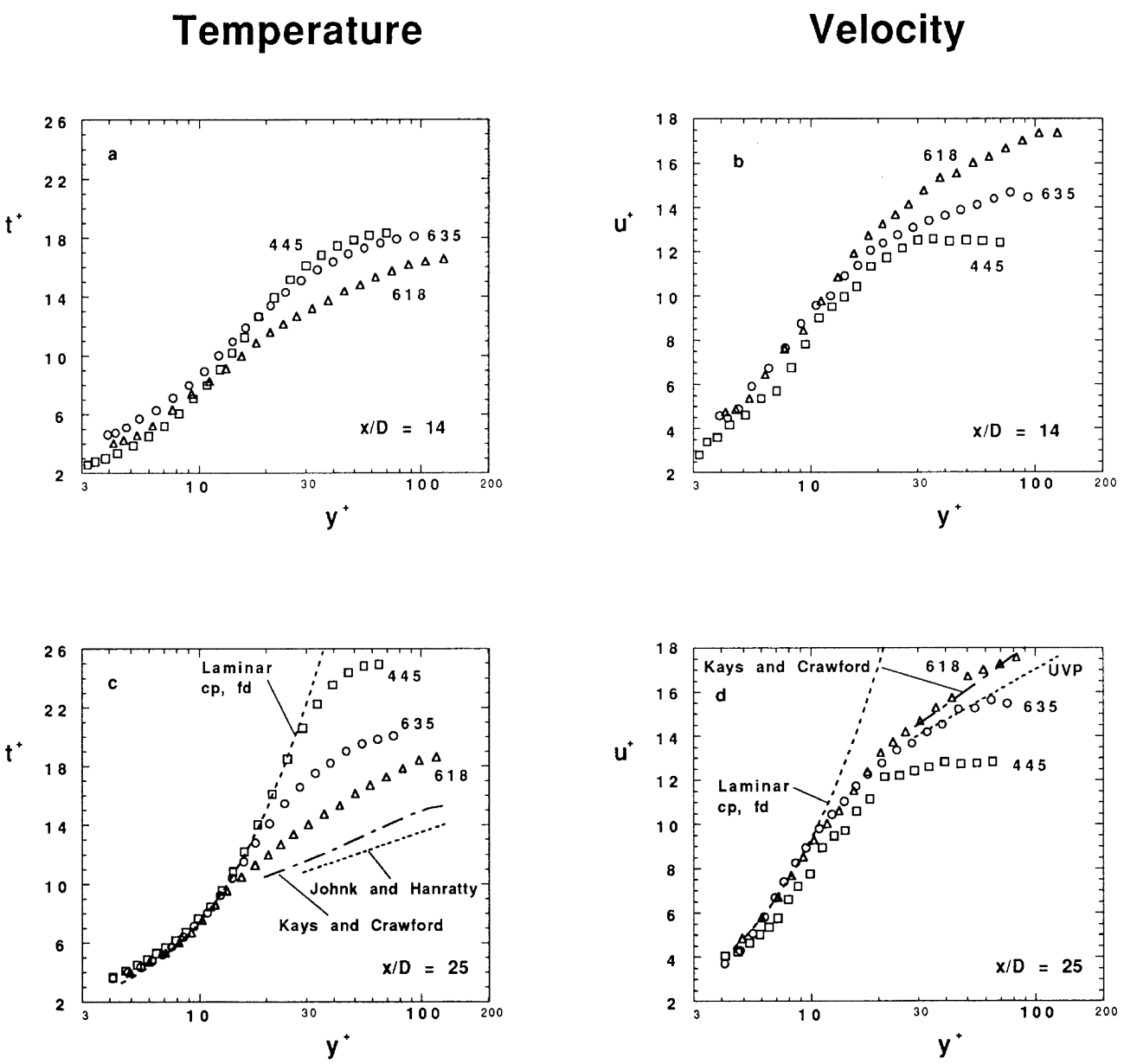

Fig. 2. Comparison of mean profiles downstream, in terms of wall coordinates.

to the thermal disturbance at the wall. Examining Run 618 (low q^+, higher Re_i), one sees evidence of a logarithmic profile beyond the viscous layer. Then as q^+ increases and Re_i decreases, the non-dimensional temperature profile $t^+\{y^+\}$ increases. Such an increase in $t^+\{y^+\}$ corresponds to a reduction in turbulent thermal energy transport with a greater fraction of $q''\{y\}$ being due to molecular transport. Comparable behavior has been observed for momentum transport in the viscous layer of flows with favorable streamwise pressure gradients [41].

The conditions at $x/D \approx 25$ (Fig. 2(c)) might be expected to be quasi-developed. The data from Run 618 are compared to the log law prediction of Johnk and Hanratty [42] and to a lower Reynolds number version presented by Kays and Crawford [35] [their equation (13.6)], with gas properties evaluated at the wall. The data are higher than either prediction; this observation is consistent with a thicker viscous layer, which would increase the thermal resistance and lower the Nusselt number as observed for heated, turbulent flows with gas property variation [6]. The fourth-order parabola for fully-established, constant-property laminar flow, $t^+ = Pr \cdot y^+ \quad [1+(0.5 \quad y/r_w)-(y/r_w)^2+0.25(y/r_w)^3]$ has been evaluated at the conditions of Run 445. At the tube center ($y_c^+ \approx 70$), $t^+\{y_c^+\}$ is predicted to be about 37. One sees agreement with this prediction for pure molecular transport to $y^+ \approx 20$–30 and then possible evidence of turbulent transport further from the wall, in the sense that $t^+\{y^+\}$ data are lower than the laminar prediction. The comparable run presented by Perkins was at slightly more severe heating conditions ($q^+ \approx 0.0055$ vice 0.0045) and gave close agreement almost to the centerline.

Run 635 temperature results fall between those of Runs 618 and 445. (For Fig. 2(a) the disagreement with the limiting behavior $t^+ \approx Pr \cdot y^+$ implies problems in the evaluation of T_w or τ_w at $x/D \approx 14$). There is an indication of less turbulent transport of thermal energy than for Run 618 and more than for Run 445. The measurements of Run 635 do not fall near either limiting prediction and there is no apparent log law region.

Mean velocity profiles $u^+\{y^+\}$ are compared to one another at $x/D \approx 14$ and 25 in Figs 2(b) and (d). As with $t^+\{y^+\}$, Run 618 has a profile shape as expected for normal fully-developed, turbulent tube flow at both locations (as well as the entering adiabatic profile). In fact, at 25 diameters the data show reasonable agreement both with the molecular transport prediction, $u^+ = (y^+/2)[1+(r/r_w)]$ at low y^+ and with a turbulent recommendation based partly on a relation for eddy viscosity by Reichardt [35, equation (11.5)] for $y^+ > \sim 30$. It is seen that the data fall above the so-called Universal Velocity Profile which was developed for high Reynolds numbers where $\tau\{y\} = \tau_w$; the approximation of Kays and Crawford accounts for $\tau\{y\}$.

At 14 diameters, Run 445 has $u^+\{y^+\}$ measurements in approximate agreement with Run 618 to $y^+ \approx 30$ (which is about one-third of the distance to the centerline) and then the profile flattens, possibly due to buoyancy forces in the thermal boundary layer. The buoyancy parameter Gr_q/Re^2 is about 0.3 at this location. The maximum velocity appears to occur between y^+ of 30 and 40 so the core region would 'see' the wall region flow as a higher velocity mixing layer, as if it were a concentric annular jet.

At 25 diameters the Run 445 profile data again agree with the higher Reynolds number run to $y^+ \approx 20$–30 ($y/r_w \approx 0.35$–0.5), then there is a sharp change in the velocity gradient—corresponding to increased turbulent transport—followed by a relatively flat central core. The buoyancy parameter Gr_q/Re^2 has decreased to about 0.2 by this location and the maximum velocity is no longer near the wall. This behavior is as one might expect for the physical entry of a pipe, with the central core accelerating uniformly with a flat profile until the momentum boundary layer grows to the center. But in the present case the turbulent velocity profile is approximately fully-developed ahead of the heating section. The high wall heat flux leads to a rapid increase in wall temperature in the axial direction and, in turn, to higher viscosity ($\mu \sim T^{0.7}$). Thus, the thermal boundary layer may appear to the oncoming turbulent flow as a slight contraction or pseudo tube entry would.

For Run 635, $u^+\{y^+\}$ shows a conventional turbulent shape at both 14 and 25 diameters and generally is intermediate between Runs 618 and 445. One could identify approximately linear near-wall layer and 'log law' regions, but the magnitudes do not agree with accepted levels for fully-developed, constant-property flows. It is difficult to establish bounds for these regions (and it may not be appropriate to examine these developing flows, with multiple phenomena, in terms of these concepts), but a possible interpretation is that the viscous layer is effectively thickened near the wall while the momentum transport is enhanced away from the wall.

The effects of significant gas property variation on the mean velocity profiles appear to differ from those on the mean temperature profiles. Whereas the temperature profiles vary as the velocity profiles of accelerated flows and drag-reducing polymer flows do, the present velocity profiles themselves do not. One may compare Figs 2(c) (temperature) and (d) (velocity), where correlations of conventional wisdom have been sketched for reference. For $t^+\{y^+\}$, as the non-dimensional heating rate becomes more severe, profiles away from the wall approach the laminar prediction with increasing values implying reduction in the turbulent transport of energy. For $u^+\{y^+\}$ an opposite result is observed: away from the wall the profiles decrease as q^+ increases, corresponding to increased turbulent transport of momentum or a trend like increasing wall roughness. The key to the apparent discrepancy may be the thermal development.

4.4. Thermal entry development

Figure 3 describes the axial flow development after the start of heating in non-dimensional terms, U/V_b and T/T_i. Symbols represent measurements while solid lines show predictions from the modified van Driest model. Wall temperature data are from the wall thermocouples while other measurements are from the wire sensor.

The first set of thermal entry data is for the 'low' heating rate conditions characterized as turbulent by Perkins [1]. The reference control parameters were $Re_i \approx 6000$ and $q^+ \approx 0.0018$ (i.e., Run 618), leading to an acceleration parameter of about 1.2×10^{-6} as shown in Fig. 1. The non-dimensional radius of the unheated upstream section is about $r^+ = y_c^+ \approx 200$. It is expected that the heat transfer parameters would correspond to turbulent predictions, with allowance for a reduction in local Nusselt number [typically of the order of $(T_w/T_b)^{-1/2}$)] due to the gas property variation along the tube and across the viscous layer.

Figure 3(a) presents the thermal and momentum development axially in terms of mean profiles at 3.17, 14.2 and 24.5 diameters. Obtaining the mean streamwise velocity data was the main objective of the present work since Perkins [1] was unable to obtain meaningful velocity measurements in his attempts with an impact tube. Velocities are normalized by the local value of the bulk velocity while the non-dimensional temperatures are based on the (absolute) inlet temperature.

Velocity profiles appear representative of normal, developed turbulent flow in a circular tube, as expected. As the flow progresses downstream, the gradient at the wall decreases with the progressive decrease in Reynolds number. No surprises are evident. For the present results a thermal boundary layer thickness is operationally defined as the distance from the wall beyond which there is no observable difference from the inlet temperature, as observed on the figures. At $x/D = 3.17$, the thermal boundary layer reached about 40% of the tube radius. By 14.2 diameters, the thermal boundary layer already extended to the centerline and the profile is typical of a developed turbulent flow, distinguished by a high gradient near the wall (most of the thermal resistance) and a well mixed flow in the interior. The last profile is qualitatively the same, with an increase in level corresponding to the higher bulk temperature. The temperature data of Perkins [1] behave in much the same way as the data in this study. Variations between the two are mainly due to minor differences in the heating rates and inlet Reynolds numbers.

The second set of data is at the intermediate heating rate (Re_i still 6000 and $q^+ \approx 0.0035$) which was described as subturbulent by Perkins [1]. The acceleration parameter was about 2×10^{-6} along most of the tube. This set has almost twice the heating rate and K_V as the first set, while having the same inlet flow rate. For these conditions, Perkins has shown that the integral heat transfer parameters do not agree with turbulent, variable properties correlations nor with laminar, variable properties numerical predictions.

Since this run is considered the most difficult of the three to model [1], mean profile data were obtained at more stations. Figure 3(b) shows the thermal development at five axial locations. The first three profiles indicate that the thermal boundary layer reached the centerline near $x/D = 9$ or 10. Near the wall the temperature profile was nearly linear over a substantial region. This region grew thicker as the flow progressed downstream, reaching $y/r_w \approx 0.25$ by the last station. Although significant thermal resistance appears distributed across a large portion of the cross-section, a near flat profile is still evident in the central region at the last three locations. This last observation implies that turbulent mixing is not suppressed there (it is not a case of being outside the thermal boundary layer, since the centerline temperature is above $T_w/T_i = 1$).

Again the velocity distribution appears to represent typical developed turbulent flow in a tube. If the normalized profiles are compared with the previous set of profiles from run 618 (in Fig. 3(a)), one sees no large differences. At $x/D \approx 3.2$ the profiles are almost coincident. Again at $x/D \approx 14.2$ they also are. Finally at the last location, run 635 is slightly more 'peaked' than run 618. That is, the (non-dimensional) gradient near the wall is lower and the central velocities are higher than for run 618. This observation is consistent with a thicker viscous layer—and with the lower local Reynolds number due to the higher heating rate. In both cases the gradients near the wall became less steep as the flow progressed downstream.

The last set of runs is at the highest non-dimensional heating rate and lowest inlet flow rate ($Re_i \approx 4000$ and $q^+ \approx 0.0045 \rightarrow$ Run 445). These conditions were categorized as being on the borderline between subturbulent and laminarizing flow by Perkins (his Fig. 8). Figure 1 shows that K_V exceeds 3.5×10^{-6}, which is considered by Sreenivasan [43] and others as near a critical value for laminarization to set in. The parameter Gr_q/Re^2 peaks at over 0.4, implying possible buoyancy effects near $x = 0$.

The measurements at 3.17 diameters (Fig. 3(c)) show that the thermal boundary layer had grown to $y/r_w \approx 0.4$ by this distance. Presumably this growth is partially a consequence of upstream axial conduction and axial thermal radiation to the tube wall of the 'unheated' entry region, as is evident earlier in Fig. 1. By $x/D = 14.2$ the thermal boundary layer again filled the tube. The temperature profile started to take a parabolic shape, except in the central region where the effects of turbulent mixing still appear significant. At $x/D = 24.5$, the measured temperature profile resembles a parabola more closely.

One recalls that the analytic profile for fully established laminar flow with constant properties is a fourth-order

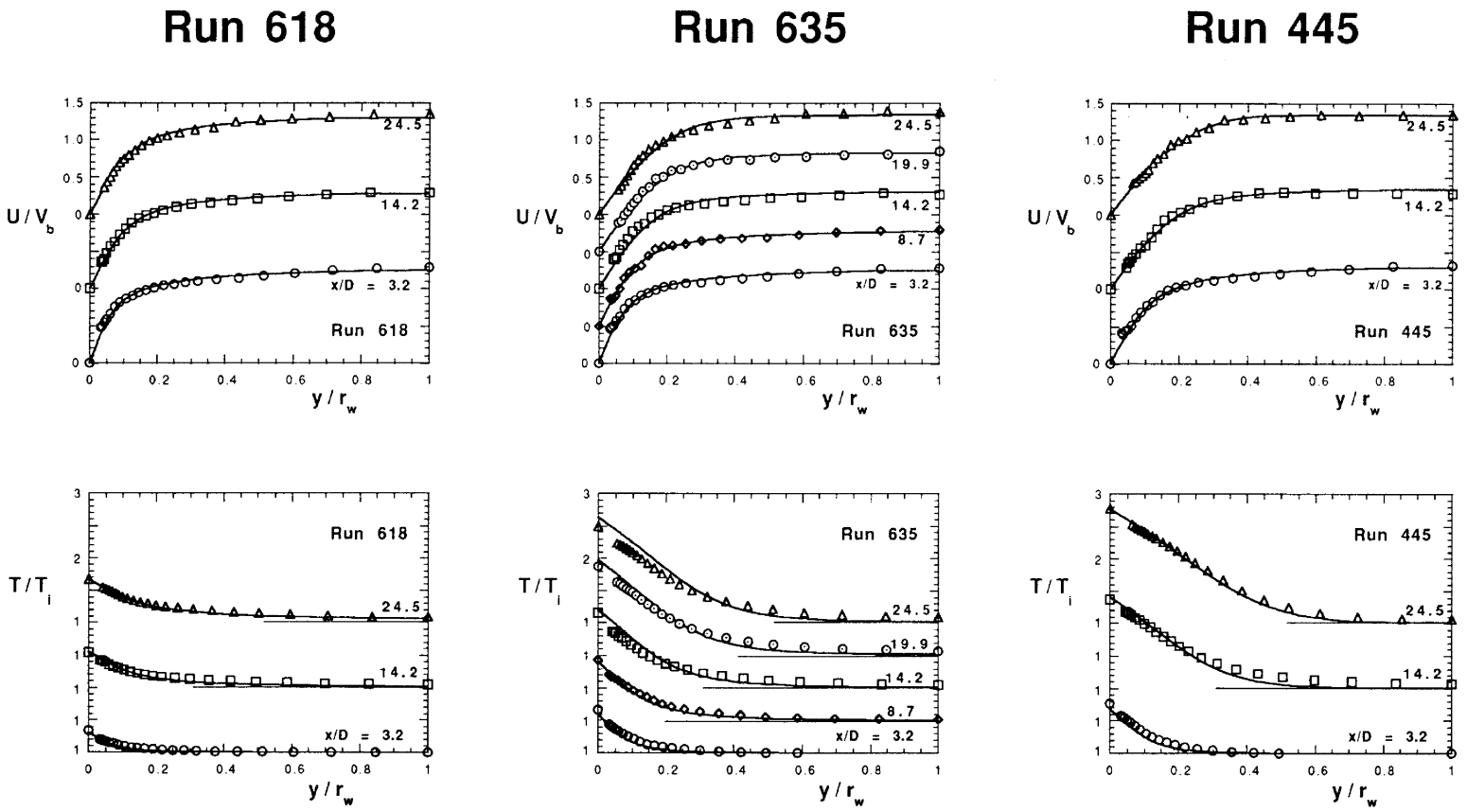

Fig. 3. Axial development of mean temperature and mean axial velocity fields. (a) 'Turbulent' run 618, $q^+ \approx 0.0018$ and $Re_{in} \approx 6080$, (b) 'subturbulent' run 635, $q^+ \approx 0.0035$ and $Re_{in} \approx 6050$, (c) 'laminarizing' run 445, $q^+ \approx 0.0045$ and $Re_{in} \approx 4260$.

parabola [35]—but, in these data, viscosity and thermal conductivity vary by factors of about two and at this Reynolds number a laminar flow would require a longer distance to become fully established. However, Perkins [1] did demonstrate that a laminar, variable properties calculation—starting from the existing turbulent velocity profile in the entry—could provide reasonable predictions of the mean temperature distribution for comparable conditions.

The mean velocity profiles in the wall region (Fig. 3(c)) show a near Blasius shape while progressing downstream. In the central region, starting at about half the radius, the profiles are almost flat for the measurements at $x/D \approx 14.2$ and 24.5, indicating high turbulent mixing, effects of acceleration, reduced shear stress and/or buoyancy effects there. The velocity profile at 14.2 diameters possesses a slightly distorted shape, consistent with buoyant forces in a heated, vertical gas flow. The velocity reaches a maximum at $y/r_w \approx 0.45$ after which it decreases to $y/r_w \approx 0.6$ and then remains approximately constant to the centerline. The local value of Gr_q/Re^2 is about 0.3 at this location. With a tube of larger diameter, Carr, Connor and Buhr [44] noticed a profile with a comparable distortion at $Gr_q/Re^2 \approx 0.46$ but at $Gr_q/Re^2 \approx 0.28$ they observed none. By using a larger tube, they reached these values with lower heating rates, i.e., less gas property variation. At the last measuring station, the velocity profile does not show an obvious maximum away from the centerline but it possesses a significant flat portion across a broad core region. The local value of Gr_q/Re^2 has decreased to below 0.2 at this position so this observation of no maximum near the wall is consistent with the data of Carr, Connor and Buhr.

The predictions from the simple, modified van Driest model agree with the profile measurements reasonably well, particularly for the runs at the highest and lowest heating rates. As found by Perkins, simulation of 'subturbulent' runs such as 635 is apparently more difficult. Wall temperature points are consistent with the results for $Nu\{x\}$ shown earlier in Fig. 5e. In Run 635 at low x/D, predictions are slightly lower than $T_w\{x\}$ data; as the flow proceeds downstream the predicted $T_w\{x\}$ profile is higher and diverges from the measurements (i.e., predicted $Nu\{x\}$ is lower and diverges further).

For Run 635, prediction of the velocity distribution appears to be better than for the temperature profiles. The poorest agreement for a velocity profile is at $x/D \approx 14.2$ where data are higher than predicted near the wall and lower in the core; these trends correspond to the temperature data being lower near the wall and higher in the central region. For temperature distributions these trends continue downstream while agreement of the velocity distribution appears to improve at $x/D \approx 20$ and 24.5. Interpreting this observation in terms of energy transport, one could say that the model predicts a lower rate of turbulent transport than observed from the wall region to the core, starting between $x/D \approx 9$ and 14; one explanation could be overprediction of the effective viscous layer thickness at these local conditions. Conceptually, one could adjust the function $A^+\{Re\}$ or other features of a turbulence model to accommodate these details (in fact, Perkins [1] did improve prediction of $T\{r, x\}$ for 'subturbulent' runs by revising $A^+\{Re\}$ at low Reynolds numbers).

4.5. Axial development of the viscous layer

A final objective of the present study is to examine the validity of the simple, modified van Driest model [10] for predicting internal flow development due to strong heating of common gases—in the viscous layer. Perkins [1] did compare predictions to his mean temperature profile data but the present study is the first opportunity to examine agreement with internal velocity distributions for dominant forced convection in this situation. Our comparisons concentrate on the viscous layer, again because it provides the dominant uncertainty in the convective thermal resistance. Also examination of profiles alone can give misleading confidence when scaled linearly on dimensions such as r_w [6, p. 157].

Figure 4 presents the comparison of predictions and data for the viscous layer in forms equivalent to wall coordinates while avoiding the uncertainty introduced by the determination of the wall shear stress. In wall coordinates the velocity profile is particularly sensitive to the uncertainty of τ_w since it appears in the numerator for y^+ and the denominator for u^+. By using the semi-log axes the presentation is concentrated on the viscous layer, e.g., for Runs 618 and 635, $y/r_w = 0.1$ corresponds to $y^+ \approx 20$ for the entering profiles. For the temperature profiles, $t_w^+ = (T_w - T)\rho_w u_{\tau,w} c_{p,w}/q''_w$ is represented by $(T_w - T)/T_i$. These comparisons of predictions and measurements are more direct (and more severe) than using wall coordinates based on a wall shear stress which has been fitted in the viscous layer.

As $t^+\{y^+\}$ normally shows the same trends as $u^+\{y^+\}$ in fully-established, constant-property flow, the profiles of $(T_w - T)/T_i$ approximate the trends of U/V_b here. This quantity also provides an indication of the variation of transport properties across the region of interest. For example, in Run 618, $(T_w - T)/T_i$ varies by about 50% to $y/r_w \approx 0.5$ so μ and k vary by about 40% in that region. In contrast, in Run 445 they vary by more within the first three diameters.

The general observations for Fig. 3 are confirmed by the comparisons of Fig. 4. Even when the examination concentrates on the near wall region, runs 618 and 445 (lowest and highest q^+) are predicted well by the modified van Driest model through the viscous layer. (At $x/D \approx 24.5$, $y_w^+ \approx 30$ corresponds to $y/r_w \approx 0.26$ for Run 618 and to $y/r_w \approx 0.5$ for 445.)

For Run 635 the velocity predictions agree reasonably

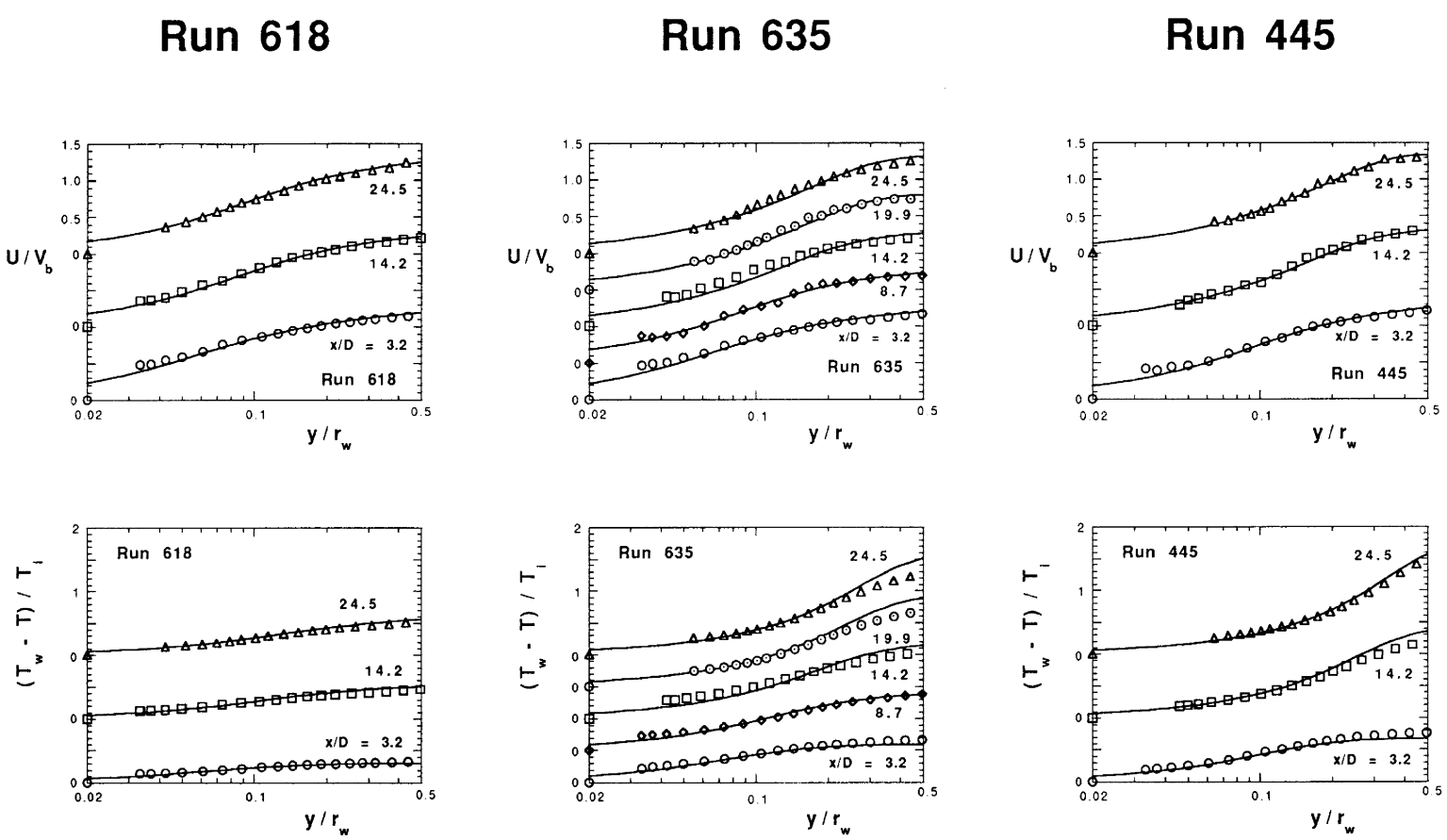

Fig. 4. Examination of axial development of viscous layer data. (a) 'Turbulent' run 618, $q^+ \approx 0.0018$ and $Re_{in} \approx 6080$, (b) 'subturbulent' run 635, $q^+ \approx 0.0035$ and $Re_{in} \approx 6050$, (c) 'laminarizing' run 445, $q^+ \approx 0.0045$ and $Re_{in} \approx 4260$.

well within the viscous layer for all but the profile at $x/D \approx 14$; at this location, $y_w^+ \approx 30$ corresponds to $y/r_w \approx 0.32$ for this run. Non-dimensional temperature profile agreement is approximately the same at this location, underpredicted for $y/r_w < \sim 0.2$ and then overestimated. Further downstream the non-dimensional temperature agrees well for $y/r_w < \sim 0.2$ then diverges for higher values. At $x/D \approx 24.5$, $y/r_w \approx 0.2$ corresponds to $y_w^+ \approx 16$, which would be about halfway across the viscous layer in unheated flow. Shehata and McEligot [31] show that $-\rho\overline{uv}/\tau_w$ is predicted to be still less than 0.1 at $x/D > 14$ at this radial position in this heated flow—so this good agreement near the wall would be a consequence of molecular transport dominating.

Figure 4(b) demonstrates that overall the modified van Driest model does correlate the mean velocity and temperature measurements fairly well even for our Run 635, the most difficult of the three to predict. As shown by Mikielewicz [23] some so-called advanced turbulence models do not do as well.

As a measure of the viscous layer thickness or a length scale for the viscous layer, we can choose the distance from the wall where ε_m is predicted to equal ν, i.e., where $\varepsilon_m/\nu = 1$ [31]. For convenience, we call this predicted location y_v^+. For the entry profile at $Re_i \approx 6000$, $y_v^+ \approx 12$ (Runs 618 and 635). For 'turbulent' Run 618, it decreases to about $11\frac{1}{2}$ and then increases to $y_v^+ \approx 14$ progressing downstream. This thickening of the viscous sublayer is consistent with empirical correlations for turbulent flow that show reductions in integral heat transfer parameters with increasing gas property variation.

In Run 635, y_v^+ is about 12 at the entry and decreases to 11 at $x/D \approx 3{,}2$ before increasing successively to 15, 27, 42 and 56 for $x/D \approx 8.7$, 14.2, 19.9 and 24.5, respectively. One might say the viscous layer, which conventionally would have significant turbulent transport from $y^+ \approx 5$–30, has laminarized although integral heat transfer parameters would not agree with laminar predictions [1]; alternatively stated, the predicted viscous layer becomes much thicker than for conventional treatments with constant properties.

Then, for Run 445, heating conditions are sufficiently severe that throughout the range of measurements ε_m/ν decreases with x. The inlet profile still represents normal turbulent flow albeit reduced compared to asymptotic high Reynolds number values, as hypothesized by McEligot et al. [45] and shown by Reynolds et al. [46]. The viscous layer length scale y_v^+ thickens continuously with x, almost reaching $y^+ = 40$ at $x/D \approx 14$. If the viscous layer is defined as the region where molecular transport is important [2], at $x/D \approx 24.5$ it extends across the entire tube. At the last station the bulk Reynolds number is about 3300. While run 635 might be considered to be laminarizing downstream, Run 445 appears to be laminarizing along the entire heated length—but it is a matter of degree. Perkins [1] has shown that the local Nusselt number for conditions like this run could be expected to agree with a laminar, variable properties correlation for the thermal entry. However, although the ε_m/ν profile shows a layer dominated by molecular viscous effects, hot wire signals showed turbulent fluctuations—apparently they are not transporting much momentum (in comparison to molecular transport). (Further details of inferred profiles of ε_m/ν, $-\rho\overline{uv}/\tau_w$ and $-\rho c_p\overline{vt}/q''_w$ are presented by Mikielewicz et al. [29] and Shehata and McEligot [31].

As seen earlier in Fig. 2, the mean velocity profile beyond $y^+ \approx 30$ becomes approximately uniform (with a possible local maximum at $x/D \approx 14.2$ and $y^+ \approx 30$) so ε_m/ν becomes near zero there in an apparently well-mixed central core. This trend would be consistent with the buoyancy effects observed by Carr et al. [44] at $Gr_q/Re_m^2 \approx 0.46$ in mixed convection with near constant properties. For our data for Run 445, Gr_q/Re_m^2 decreases from ~ 0.4–~ 0.2 over the distance from $x/D \approx 6 \rightarrow 25$.

5. Concluding remarks

The viscous layer in gaseous, turbulent tube flow with strong heating, but dominant forced convection, has been probed via thermal anemometry. Experiments for air flowing upward in a vertical circular tube were conducted for heating rates causing significant property variation after an unheated entry of 50 diameters, preceding the heating. Two entry Reynolds numbers of approximately 6000 and 4000 were employed—concentrating on three heating rates, $q^+ \approx 0.0018$, 0.0035 and 0.0045, to give conditions considered to be 'turbulent', 'subturbulent' and close to 'laminarizing', respectively. The acceleration parameters and buoyancy parameters were significant with ranges of $1.2 \times 10^{-6} < K_V < 4.1 \times 10^{-6}$ and $0.1 < Gr_q/Re_m^2 < 0.53$, respectively. Examination emphasizes the wall region which would conventionally be expected to contain the viscous layer, $0 < y^+ < \sim 30$, if the flow were unheated.

Development was measured by obtaining internal mean axial velocity and temperature profiles at axial stations from about 3.2–24.5 diameters. Prior to the present measurements, data for mean velocity distributions were not available for this situation. As described by Shehata and McEligot [31], these measurements required a substantial development effort and calibration to account for the effects of large temperature differences on the thermal anemometry employed.

Until these data became available, 'advanced turbulence models' for internal flow with variable properties (e.g., Kawamura [12], Fujii et al. [18], Torii et al. [21], Torii and Yang [20]) have not even had mean velocity profiles to verify or refute their assumptions for the viscous layer and comparisons by Mikielewicz [23] have

shown that most advanced turbulence models are refuted for these conditions.

In these flows the thermal boundary layer reached the centerline by about 14 diameters. At the higher Reynolds number and the lowest heating rate (called 'turbulent' above), after being disturbed in the first few diameters by the heating and its accompanying property variation, profiles representing the turbulence quantities—l/y, ε_m/ν, $-\rho\overline{uw}/\tau_w$ and $-\rho c_p\overline{vt}/q''_w$—appear to recover to approximately self-preserving conditions as shown separately by Shehata and McEligot [31]. In the other two runs with higher heating rates, these turbulence quantities decrease after the entrance until they are small relative to molecular effects.

In addition to documenting the first mean velocity distributions for these difficult cases, the present study demonstrated that the simple modified van Driest model (developed from wall data alone by McEligot and Bankston [10]) predicts the mean internal profiles and nondimensional pressure drop reasonably well overall. However, Bates et al. [15] have demonstrated that this model is not appropriate for flows with large buoyancy effects.

Acknowledgements

The study reported was partly supported through the Laboratory Directed Research and Development Program and the Long Term Research Initiative Program of EG&G Idaho and Lockheed Martin Idaho Technologies Company under DoE Idaho Operations Office Contracts DE-AC07-76ID01570 and DE-AC07-94ID13223, respectively. Earlier incarnations were financed by the National Science Foundation (Dr Win Aung, Program Manager), the Office of Naval Research (Mr M. Keith Ellingsworth, Program Manager) and the Aerospace and Mechanical Engineering Department of the University of Arizona while the authors were at the University of Arizona. To all we are extremely grateful. By acceptance of this article for publication, the publisher recognizes the U.S. Government's (license) rights in any copyright and the Government and its authorized representatives have unrestricted right to reproduce in whole or in part said article under any copyright secured by the publisher.

References

[1] Perkins KR. Turbulence structure in gas flows laminarizing by heating. Ph.D. thesis, University of Arizona, 1975.
[2] Bradshaw P. An introduction to turbulence and its measurement. New York : Pergamon, 1971.
[3] Reiss LP, Hanratty TJ. An experimental study of the unsteady nature of the viscous sublayer. AIChE Journal 1963;9:154–60.
[4] Narasimha R, Sreenivasan KR. Relaminarization of fluid flows. Adv Appl Mech 1979;19:221–309.
[5] Perkins HC, Worsoe-Schmidt PM. Turbulent heat and momentum transfer for gases in a circular tube at wall-to-bulk temperature ratios to seven. Int J Heat Mass Transfer 1965;8:1011–31.
[6] McEligot DM. Convective heat transfer in internal gas flows with temperature-dependent properties. Adv Transport Processes 1986;4:113–200.
[7] Humble LV, Lowdermilk WH, Desmon LG. Measurements of average heat-transfer and friction coefficients for subsonic flow of air in smooth tubes at high surface and fluid temperatures. NACA Report 1020, 1951.
[8] Jackson JD. A theoretical investigation into the effects of surface/gas temperature ratio for fully developed turbulent flow of air, helium and carbon dioxide in smooth circular tubes. A.R.C. 22, 784, F.M. 3084 (U.K.), 1961. Also ASTIA AD-269 066.
[9] McEligot DM, Magee PM, Leppert G. Effect of large temperature gradients on convective heat transfer : the downstream region. J Heat Transfer 1965;87:67–76.
[10] McEligot DM, Bankston CA. Turbulent predictions for circular tube laminarization by heating. ASME paper 69-HT-52, 1969. Available from Engineering Societies Library, New York.
[11] Bankson CA, McEligot DM. Turbulent and laminar heat transfer to gases with varying properties in the entry region of circular ducts. Int J Heat Mass Transfer 1970;13:319–344. Also Technical Report LA-4149, Los Alamos Scientific Laboratory, 1969.
[12] Kawamura H. Analysis of laminarization of heated turbulent gas using a two-equation model of turbulence. Proc 2nd Intl Symp Turb Shear Flow, London, 1979, pp. 18.16–21.
[13] van Driest ER. On turbulent flow near a wall. J Aerospace Sci 1956;23:1007–11 and 1036.
[14] Perkins KR, McEligot DM. Mean temperature profiles in heated laminarizing air flows. J Heat Transfer 1975;97:589–93.
[15] Bates JA, Schmall RA, Hasen GA, McEligot DM. Effects of buoyant forces on forced convection in heated laminarizing flows. Proc. 5th Int Heat Transfer Conf II, 141–5, 1974.
[16] Ogawa M, Kawamura H, Takizuka T and Akino N. Experiment on laminarization of strongly heated gas flow in a vertical circular tube. J At Energy Soc, Japan 1982;24(1):60–7.
[17] Ogawa M, Kawamura H. Experimental and analytical studies on friction factor of heated gas flow in circular tube. J At Energy Soc, Japan 1986;28(10):957–65 (in Japanese).
[18] Fujii S, Akino N, Hishida M, Kawamura H, Sanokawa K. Experimental and theoretical investigations on heat transfer of strongly heated turbulent gas flow in an annular duct. JSME International J, Ser II 1991;34(3):348–54.
[10] Torii S, Shimizu A, Hasegawa S, Kusama N. Laminarization of strongly heated gas flows. JSME International J, Ser II 1991;34(2):157–68.
[20] Torii S, Yang W-J. Laminarization of gas flows inside a strongly heated tube. Int J Heat Mass Transfer 1997;40:3105–7.
[21] Torii S, Shimizu A, Hasegawa S, Higasa M. Numerical

analysis of laminarizing circular tube flows by means of a Reynolds stress turbulence model. Heat Transfer—Japanese Research 1993;22:154–70.
[22] Launder BE, Shima N. Second-moment closure for the near-wall sublayer : development and application. AIAA J 1989;27:1319–25.
[23] Mikielewicz DP. Comparative studies of turbulence models under conditions of mixed convection with variable properties in heated vertical tubes. Ph.D. thesis, University of Manchester, 1994.
[24] Ezato K, Shehata AM, Kunugi T, McEligot DM. Numerical predictions of transitional features of turbulent gas flows in circular tubes with strong heating. ASME paper FEDSM97-3304, presented at ASME Fluids Engineering Conf, Vancouver, BC, 1997. Accepted for J Heat Transfer, pending revisions.
[25] Nishimura M, Fujii S, Shehata AM, Kunugi T, McEligot DM. Prediction of forced gas flows in circular tubes at high heat fluxes. Presented at NuReTH-8, Kyoto, 1997.
[26] Shehata AM. Mean turbulence structure in strongly heated air flows. Ph.D. thesis, University of Arizona, 1984.
[27] Nash JF, MacDonald AGJ. A calculation method for incompressible turbulent boundary layers including the effect of upstream history on the turbulent shear stress. NPL Aero Report 1234, 1967. Also NASA N68-20516.
[28] Reynolds HC, Swearingen TB, McEligot DM. Thermal entry for low-Reynolds-number turbulent flow. J Basic Engrg 1969;91:87–94.
[29] Mikielewicz DP, Shehata AM, Jackson JD, McEligot DM. Temperature, velocity and mean turbulence structure in strongly-heated internal gas flows. Comparison of numerical predictions with data. Under revision for Int J Heat Mass Transfer.
[30] McEligot DM, Taylor MF. The turbulent Prandtl number in the near-wall region for low-Prandtl-number gas mixtures. Int J Heat Mass Transfer 1996;39:1287–95.
[31] Shehata AM, McEligot DM. Turbulence structure in the viscous layer of strongly heated gas flows. Tech. report INEL-95/0223, Idaho National Engineering Laboratory, 1995.
[32] Schlichting H. Boundary layer theory. 6th ed. New York : McGraw-Hill, 1968.
[33] Drew TB, Koo EC, McAdams WM. The friction factor in clean round pipes. Trans AIChE 1932;38:56–72.
[34] Kline SJ, McClintock FA. Describing uncertainties in single-sample experiments. Mech Engr 1953;75(1):3–8.
[35] Kays WM, Crawford ME. Convective heat and mass transfer. 2nd ed. New York : McGraw-Hill, 1980.
[36] Kline SJ, Reynolds WC, Schraub FA, Rundstadler PW. The structure of turbulent boundary layers. J Fluid Mech 1967;30:741–73.
[37] Chambers FW, Murphy HD, McEligot DM. Laterally converging flow. Part 2. Temporal wall shear stress. J Fluid Mech 1983;127:403–28.
[38] McEligot DM, Swearingen TB. Predictions of wall temperatures for internal laminar heat transfer. Int J Heat Mass Transfer 1966;9:1151–2.
[39] Shumway RW. Variable properties laminar gas flow heat transfer and pressure drop in annuli. Ph.D. thesis, University of Arizona, 1969. Also DDC-AD-696 0458.
[40] Shumway RW. Personal communication. Idaho National Engineering Laboratory, 1993.
[41] McEligot DM, Eckelman H. Turbulence structure in the viscous layer of converging flows. Proc 9th Intl Symp Turb shear flows, Kyoto, 1993;1:8-5-1–6.
[42] Johnk RE, Hanratty TJ. Temperature profiles for turbulent flow of air in a pipe. Chem Eng Sci 1962;17:867–92.
[43] Sreenivasan KR. Laminarescent, relaminarizing and retransitional flows. Acta Mechanica 1982;44:1–48.
[44] Carr AD, Connor MA, Buhr HO. Velocity, temperature and turbulence measurements in air pipe flow with combined free and forced convection. J Heat Transfer 1973;95:445–52.
[45] McEligot DM, Ormand LW, Perkins HC. Internal low Reynolds number turbulent and transitional gas flow with heat transfer. J Heat Transfer 1966;88:239–45.
[46] Reynolds HC, Davenport ME, McEligot DM. Velocity profiles and eddy diffusivities for fully developed turbulent, low Reynolds number pipe flow. ASME Paper 68-WA/FE-34, 1968.